A novel location awareness method for spot beam emitters

Weicai Yang [1*], Qing Chang [1], Hui Li [2], Yang Gao[3], Lina Bao[4]

[1] School of Electronic and Information Engineering, Beihang University, Xueyuan Road No. 37 Haidian District,Beijing, China
[2] Spacekey Technology Company Ltd., Beijing, China
[3] State Key Laboratory of Virtual Reality Technology and Systems, Beihang University, Beijing, China
[4] Tianjin University, Tianjin, China
[*] kaka2008666@126.com

Abstract: As more and more spacecraft launched into the space, the probability of radiofrequency (RF) interference raises and the burden of RF spectrum management increases as well. The monitoring of global RF beam information and identifying of spot beam emitters location can effectively obtain space data resources, which will do great help for mitigating global RF interference and optimizing space spectrum resources. This paper proposes a novel location awareness method for spot beam emitters based on the nanosatellite platform. The proposed method identifies the position of spot beam emitters on a global scale by flying a low earth orbit CubeSat constellation through the coverage of the spot beams. The properties such as geometry, the target motion equation, the measurement process and the Particle Filter equations are all addressed with respect to the location methods. We illustrate a realistic scenario simulated within the Systems Tool Kit, in which CubeSats receive signals from the spot beam emitters. The scenario shows that our location awareness method proposed in this paper is available and efficient.

1. Introduction

The current and future strategic environment is driven by three trends - space is becoming increasingly congested, contested, and competitive [1]. As more and more spacecraft launched into the space, the probability of radiofrequency (RF) interference raises and the burden of RF spectrum management increases as well. The Satellite Interference Reduction Group and Space Data Association discover that RF interference has seriously affected satellite communication in the past years [2, 3]. The monitoring of global RF beam information and identifying of spot beam emitters location can effectively obtain space data resources. It will do great help for mitigating global RF interference and optimizing space spectrum resources.

To verify and monitor the use of global satellites RF signal, traditional approaches always take advantage of a wideband spectrum receiver at a fixed ground station terminal [4]. Although satellite signals can be measured in this manner, the ground map data is just used for a single region ground point. Furthermore, the ground monitoring stations are difficult to be deployed in the extreme areas such as ocean and polar region. Therefore, the traditional ground monitoring methods are difficult to fulfill the task of global RF monitoring. In order to overcome the above-mentioned difficulties, a CubeSat mission was recently proposed as an effective way to verify the RF signal of satellites [5]. The CubeSat mission would carry out the verification by mapping spot beams from low earth orbit (LEO), making it possible to establish a monitoring station with no territorial limitation. Moreover, this method generates a beam pattern database with higher resolution than the fixed ground site measurements. GOMspace conducts a new innovation called BeamWatch, which is designed based on a similar idea. The project contains the development and testing of a nanosatellite prototype, which is designed to predict and measure the quality of communication from more than 400 communication satellites with a critical part of the modern global communication infrastructure [6]. Unfortunately, [5] and [6] could not propose an appropriate method to identify the emitter’s location. In view of the above problems, this paper aims to propose a novel efficient method which can identify the location of the spot beam emitters on a global scale to overcome the drawbacks of existing methods. Our location awareness method for spot beam emitter is based on the nanosatellite platform. It will be helpful for locating the source of interference and managing the operation of spacecraft.

At the algorithm level, passive target localization and tracking with a single moving observer is a widely studied estimation problem. If the observer-to-target angles and/or the Doppler-shifted emitter frequencies are measured, depending on the type of measurements used, three different tracking procedures can be distinguished: angle-only tracking (AOT), frequency-only tracking (FOT), and angle/frequency tracking (AFT). AOT is the standard method used in passive target tracking, and it has been the topic of much research in the literature [7-10]. In order to improve the localization accuracy, a variety of filtering algorithms have been proposed [11-14]. In comparison with the literature dealing with the AOT problem, the number of publication analysis FOT [15, 16] and AFT [17-21] is substantially smaller. An alternative recursive Bayesian tracking approach is to employ the Particle Filter (PF) which has recently become popular in the nonlinear filtering literature [22-25]. The Particle Filter, whose principal idea is to use of Monte Carlo simulation to implement Bayesian recursive filters, is an effective method for the treatment of nonlinearity and non-gaussianity. This paper presents a study of the particles filter in location awareness of the space spot beam emitter using angle and frequency measurements. The salient contributions of this paper are summarized as:

•The proposed location awareness method uses a single CubeSat with angles and frequencies measurements to identify the position of the spot beam emitters.

•The properties such as geometry, the target motion equation, the measurement process and the Particle Filter equations are all addressed with respect to the location methods.

•To show the accuracy of our proposed method, a realistic scenario simulated within the STK is designed, in which CubeSats receive signals from the spot beam emitters.

•Furthermore, angle-only and frequency-only measurements are analyzed and compared, which provides sufficient theoretical analysis for designing the CubeSat payload.

The framework of our work is organized as follows: Section 2 presents the formulation of the spot beam emitter location awareness. Section 3 focuses on simulation of the location awareness scene of the spot beam emitters. In Section 4, the performance of positioning is analyzed based on the simulated scene. Finally, concluding remarks are provided in Section 5.

2. Problem Formuhlation

In this section, we first describe the geometry used in the spot beam emitter location awareness. Then, we briefly discuss about the target motion and the measurement process associated with the onboard sensor. Finally, we propose our PF estimation algorithm which is applied to estimate the position of spot beam emitters.

2.1. Geometry for Spot Beam Emitter Location Awareness

In this paper, a novel approach that involves flying a CubeSat through spot beams of an emitter at the altitude of an LEO is adopted to identify the location of the spot beam emitter. As depicted in Fig. 1, which is the illustration of location awareness method of a spot beam emitter.

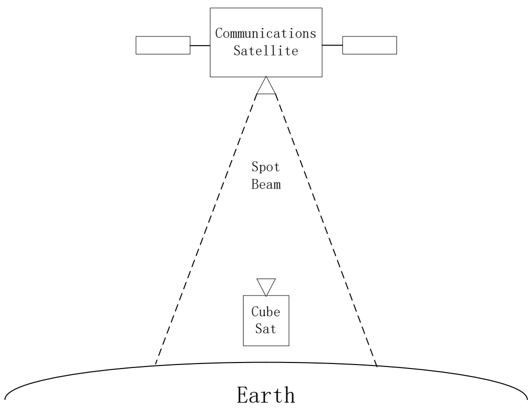

Fig. 1 the location awareness method of a spot beam emitter.

The model for the location awareness system is set up in the standard J2000 earth centered inertial reference frame. The communications satellite with the spot beam emitter and the CubeSat are regarded as two independent particles which move under the force of Earth's gravity. The geometric configuration is given in Fig. 2.

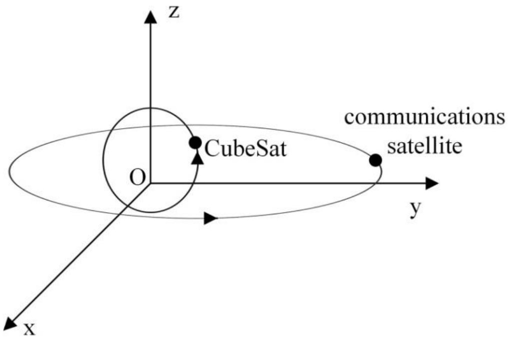

Fig. 2 Geometry of the location awareness system.

Here, the position and velocity vectors for the spot beam emitter are expressed as $\boldsymbol{r_e} = (x_e, y_e, z_e)$ and $\boldsymbol{v_e} = (v_{x_e}, v_{y_e}, v_{z_e})$ respectively. The corresponding vectors for the CubeSat are expressed as $\boldsymbol{r_{cub}} = (x_{cub}, y_{cub}, z_{cub})$ and $\boldsymbol{v_{cub}} = (v_{x_{cub}}, v_{y_{cub}}, v_{z_{cub}})$.

2.2. The equations of motion for target spot beam emitter

The equation of motion for the orbiting satellites is governed by Kepler's two-body equation, which is expressed as follows [26]

$$\boldsymbol{a} = -\frac{\mu}{r^2}\cdot\frac{\boldsymbol{r}}{r} \quad (1)$$

where $\boldsymbol{a} = (a_x, a_y, a_z)$ is the three-dimensional acceleration vector of the satellite, $\boldsymbol{r} = (x, y, z)$ is the satellite's position vector, and r is a scalar that denotes the distance between the satellite and the center of Earth, μ is the geocentric gravitational constant, the value of which is approximately equal to $3.986004415\times 10^{14}\ \mathrm{m^3/s^2}$, according to criterion of the International Astronomical Union (IAU).

The motion parameters of the target spot beam emitter at time $t = iT$, $i = 1, 2, 3, \ldots$ (T denotes the sampling interval) can be calculated by the following iterative method

$$\boldsymbol{r}_{\boldsymbol{e}_i} = \boldsymbol{r}_{\boldsymbol{e}_{i-1}} + \boldsymbol{v}_{\boldsymbol{e}_{i-1}}\cdot T + \boldsymbol{a}_{\boldsymbol{e}_{i-1}}\cdot\frac{T^2}{2} \quad (2)$$

$$\boldsymbol{v}_{\boldsymbol{e}_i} = \boldsymbol{v}_{\boldsymbol{e}_{i-1}} + \boldsymbol{a}_{\boldsymbol{e}_{i-1}}\cdot T \quad (3)$$

$$\boldsymbol{a}_{\boldsymbol{e}_i} = -\frac{\mu}{{r_e}^2}\cdot\frac{\boldsymbol{r}_{\boldsymbol{e}_i}}{r_e} \quad (4)$$

Furthermore, the state vector of the target can be derived as follows:

$$\boldsymbol{X}_i = \boldsymbol{X}_{i-1} + \dot{\boldsymbol{X}}_{i-1}\cdot T + B\cdot\dot{\boldsymbol{X}}_{i-1}\cdot\frac{T^2}{2} \quad (5)$$

where X=[$x_e\ y_e\ z_e\ v_{x_e}\ v_{y_e}\ v_{z_e}$]' is a six-dimensional state vector that describes the position and velocity of the target, the "prime" symbol (') denoting matrix transposition. $\dot{X}$ = [$v_{x_e}\ v_{y_e}\ v_{z_e}\ a_{x_e}\ a_{y_e}\ a_{z_e}$]' is the derivative of X, and

$$B = \begin{bmatrix} O & I \\ O & O \end{bmatrix},$$

where I is a 3×3 identity matrix and O is a 3×3 null matrix.

2

Substituting Eq. (1) into Eq. (5) yields the expression for the state model of the target as follows

$$\boldsymbol{X}_i = \begin{bmatrix} 1-\frac{\mu}{r^3}\cdot\frac{T^2}{2} & 0 & 0 & T & 0 & 0 \\ 0 & 1-\frac{\mu}{r^3}\cdot\frac{T^2}{2} & 0 & 0 & T & 0 \\ 0 & 0 & 1-\frac{\mu}{r^3}\cdot\frac{T^2}{2} & 0 & 0 & T \\ -\frac{\mu}{r^3}\cdot T & 0 & 0 & 1 & 0 & 0 \\ 0 & -\frac{\mu}{r^3}\cdot T & 0 & 0 & 1 & 0 \\ 0 & 0 & -\frac{\mu}{r^3}\cdot T & 0 & 0 & 1 \end{bmatrix}\boldsymbol{X}_{i-1} = A_{i-1}\boldsymbol{X}_{i-1} \quad (6)$$

It should be noted that Eq. (6) is derived with the assumption that the target's acceleration is constant between the two samplings.

2.3. Measurement Process

To obtain a measurement for the spot beam emitter, it is quite necessary to have an angle measuring sensor onboard the CubeSat and to obtain the position information of the CubeSat. The location awareness CubeSat, during a notional orbit, is expected to physically fly through a large number of spot beams with coverage areas of various sizes. Once the emitter signal is detected, the CubeSat with an angle sensor measures azimuth and elevation angles of the incoming signals and estimates the frequency value of the received signal. At the same time, the CubeSat outputs its own position and velocity. The position and velocity of the CubeSat can be obtained from the GPS receiver mounted on it [27]. Fig. 3 shows the overall azimuth and elevation angles of the CubeSat with respect to the target emitter. The angles and frequencies are given by the equations (7-9).

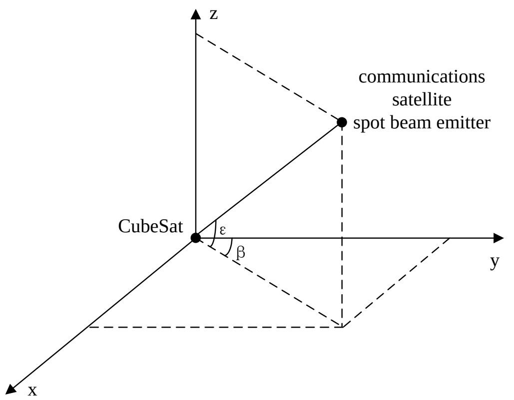

Fig. 3 Overall emitter and CubeSat geometry showing azimuth and elevation angles.

$$\beta = tan^{-1}\left(\frac{x_e - x_{cub}}{y_e - y_{cub}}\right) + \delta_\beta (7)$$

$$\varepsilon = tan^{-1}\left(\frac{z_e - z_{cub}}{\sqrt{(x_e - x_{cub})^2 + (y_e - y_{cub})^2}}\right) + \delta_\varepsilon \ (8)$$

$$f = f_0 + f_d = f_0\left(1 - \frac{(\boldsymbol{v_e} - \boldsymbol{v_{cub}})\cdot(\boldsymbol{r_e} - \boldsymbol{r_{cub}})}{c||\boldsymbol{r_e} - \boldsymbol{r_{cub}}||}\right) + \delta_f \ (9)$$

In equations (7-9), δ_β, δ_ε and δ_f are assumed to be mutually independent zero-mean Gaussian white noise. f represents the frequency value of the received signal, while f_0 is unknown emitting signal carrier frequency and f_d is doppler frequency shift.

The measurement matrix defined by Eq. (10) is a nonlinear problem.

$$z = \begin{bmatrix} \beta \\ \varepsilon \\ f \end{bmatrix} = h(\boldsymbol{X}) \ (10)$$

Therefore, the nonlinear filter algorithm is quite necessary and convenient to estimate the position of the spot beam emitter in a simple and efficient manner.

2.4. Particle Filter

The Particle Filter is a normal technique for implementing a recursive Bayesian filter by Monte-Carlo simulations. The principal idea of this algorithm is to represent the posterior density for a set of weighted random samples and to estimate the parameters of interest based on these samples and weights.

Select the position, velocity and signal frequency of the spot beam emitter as the state vector $\boldsymbol{X_{AFT}}$:

$$\boldsymbol{X_{AFT}} = [x_e \ y_e \ z_e \ v_{x_e} \ v_{y_e} \ v_{z_e} \ f_0]' \ (11)$$

Let $\{X_{AFT}{}_i^k, q_i^k\}_{k=1}^N$ denote a sample set that characterizes the posterior probability density function (pdf) $p(X_{AFT}{}_i|Z_i)$, where $X_{AFT}{}_i^k$, $k = 1, \ldots, N$, is a set of sample points with associated weights q_i^k, N is the total number of particles. $Z_i = \{z_k : k = 1, \ldots, i\}$ is the set of measurements at time step i. The posterior density can be approximated by

$$p(\boldsymbol{X_{AFT}}_i|Z_i) \approx \sum_{k=1}^{N} q_i^k \delta(\boldsymbol{X_{AFT}}_i - \boldsymbol{X_{AFT}}_i^k) \ (12)$$

where $\delta(\cdot)$ is the Dirac function, the initial $X_{AFT}{}_0^k \sim p(X_{AFT}{}_0)$ and initial weights $q_0^k = 1/N$.

Each sample is passed by the dynamic equation (13) to obtain the prior of the state at time step i,

$$\hat{\boldsymbol{X}}_{\boldsymbol{AFT}_i}^k = \boldsymbol{A_{AFT}}_{i-1}\boldsymbol{X_{AFT}}_i^k + \boldsymbol{W_{i-1}} \ (13)$$

where $\hat{\boldsymbol{X}}_{\boldsymbol{AFT}_i}^{\boldsymbol{k}}$ represents a prior of the true state vector $\boldsymbol{X_{AFT}}_i^k$, and the error sequences described by $\boldsymbol{W}_i$. The transition matrix $\boldsymbol{A_{AFT}}_{i-1}$ can be written as:

$$\boldsymbol{A_{AFT}} = \begin{bmatrix} 1-\frac{\mu}{r^3}\cdot\frac{T^2}{2} & 0 & 0 & T & 0 & 0 & 0 \\ 0 & 1-\frac{\mu}{r^3}\cdot\frac{T^2}{2} & 0 & 0 & T & 0 & 0 \\ 0 & 0 & 1-\frac{\mu}{r^3}\cdot\frac{T^2}{2} & 0 & 0 & T & 0 \\ -\frac{\mu}{r^3}\cdot T & 0 & 0 & 1 & 0 & 0 & 0 \\ 0 & -\frac{\mu}{r^3}\cdot T & 0 & 0 & 1 & 0 & 0 \\ 0 & 0 & -\frac{\mu}{r^3}\cdot T & 0 & 0 & 1 & 0 \\ 0 & 0 & 0 & 0 & 0 & 0 & 1 \end{bmatrix} (14)$$

On receipt of the measurement z_i, compute the likelihood $p(z_i|\boldsymbol{X_{AFT}}_i^k)$ of each prior sample

$$p(z_i|\boldsymbol{X_{AFT}}_i^k) = p(\beta_i|\boldsymbol{X_{AFT}}_i^k) \cdot p(\varepsilon_i|\boldsymbol{X_{AFT}}_i^k) \cdot p(f_i|\boldsymbol{X_{AFT}}_i^k)$$

$$= \frac{1}{\sqrt{2\pi\sigma_\beta^2}} exp\left[-\frac{1}{2}\left(\frac{\beta_i-\hat{\beta}_i^k}{\sigma_\beta}\right)^2\right] \cdot \frac{1}{\sqrt{2\pi\sigma_\varepsilon^2}} exp[-\frac{1}{2}(\frac{\varepsilon_i-\hat{\varepsilon}_i^k}{\sigma_\varepsilon})^2] \cdot$$

$$\frac{1}{\sqrt{2\pi\sigma_f^2}} exp[-\frac{1}{2}(\frac{f_i-\hat{f}_i^k}{\sigma_f})^2] \quad (15)$$

where σ_β , σ_ε and σ_f are the standard deviation of measurement, $\hat{\beta}_i^k$, $\hat{\varepsilon}_i^k$ and $\hat{f}_i^k$ are computed by the prior sample.

Update the weights by

$$q_i^k = q_{i-1}^k \frac{\mathrm{p}(z_i|\mathbf{X_{AFT}}_i^k)\mathrm{p}(\mathbf{X_{AFT}}_i^k|\mathbf{X_{AFT}}_{i-1}^k)}{\mathrm{p}(\mathbf{X_{AFT}}_i^k|\mathbf{X_{AFT}}_{i-1}^k, Z_i)} \quad (16)$$

In this application, we use the optimal importance density $p(\boldsymbol{X_{AFT}}_i^k|\boldsymbol{X_{AFT}}_{i-1}^k, Z_i) \approx p(\boldsymbol{X_{AFT}}_i^k|\boldsymbol{X_{AFT}}_{i-1}^k)$. Then, the updated weights become

$$q_i^k = q_{i-1}^k \, \mathrm{p}(z_i|\mathbf{X_{AFT}}_i^k) \quad (17)$$

Normalize the weights as follows

$$q_i^k = \frac{q_i^k}{\sum_{k=1}^N q_i^k} \quad (18)$$

Thus, the state vector at time step i can be calculated by

$$\boldsymbol{X_{AFT}}_i = \sum_{k=1}^N q_i^k \hat{\boldsymbol{X}}_{\boldsymbol{AFT}_i}^k \quad (19)$$

A common problem with the PF should be note is the degeneracy phenomenon. After a few iterations, some particles have negligible weight. The degeneracy phenomenon can be empirically evaluated by

$$N_{eff} = \frac{\mathbf{1}}{\sum_{k=1}^N \boldsymbol{q_i^k}^2} \quad (20)$$

The small N_{eff} indicates severe degeneracy. To overcome the problem, a resampling method is adopted. Resampling can be performed when N_{eff} is below threshold N_{thres}. The Resampling involves generating a new set $\{X_{AFT}{}_i^k\}_{k=1}^N$ and resetting the weights $q_i^k = \frac{1}{N}$.

3. Model Simulation

As discussed in the previous section, the problem is locating the spot beam emitters with CubeSats in LEO. The location awareness process was modeled using the Systems Tool Kit (STK) to simulate a scene in which CubeSats receive signals from spot beam emitters. In order to verify whether the algorithm is suitable for spot beam emitters with different orbits, two communications satellites with different orbits are selected in the simulation scene. The measurement data and the CubeSat's position obtained from the simulation scene.

The Intelsat Galaxy 28 (G-28) was modeled as the first geosynchronous orbit communications satellite. The G-28 satellite maintains spot beams emitters within the C-band, the Ku-band and the Ka-band [28]. Since the coverage of the Ku-band spot beam is smaller than that of the C-band, it can provide better performance verification for the proposed location awareness algorithm. Therefore, the Ku-band and the Ka-band spot beam emitters were modeled on the G-28 satellite. Since most companies do not publish exact antenna due to their proprietary nature, typical antenna sizes for the simulated K-band beams are assumed in accordance with [29]. For this research, the simulated Ku-band and Ka-band antennas were assumed to be 1 m diameter. The Ku-band beams frequency was set to be 12 GHz, which is approximately the downlink frequency used by the G-28 emitter [28]. To model the beams accurately, half-power sensors were combined to notionally match the conical shape. The highest frequency portion of the Ka-band (40 GHz) was used in the Ka-band emitter model. The AMSC1 satellite was created on an inclined orbit as the second communication satellite. The Ku-band frequency of the AMSC1 satellite was set to 11GHz.

CubeSats fly on LEO as monitoring satellite. In order to achieve the optimum mapping of the spot beams, the orbit parameters of CubeSats were designed in paper [5]. For this study, we use the results of the paper [5] and summarize the results in Table 1. Four CubeSats were used to monitor the Ku-band signals, and the other four CubeSats were used to monitor the Ka-band signals. It must be noted that multiple CubeSats were modeled to increase the responsiveness and shorten the necessary data collection duration. However, in the location-awareness process, any CubeSat can locate a spot beam emitter alone. Finally, the location awareness scene of the spot beam emitter is shown in Figure 4.

Table 1 Constraints for the CubeSat constellations and orbits

Constellation Altitude:	400 km
Constellation Inclination:	68 degrees
Payload Sampling Rate:	1 s per sample
Number of Orbit Planes:	1 plane
Number of CubeSats in Plane:	8 satellites
CubeSat Spacing within Plane	Evenly spaced

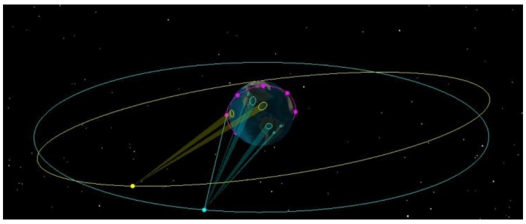

Fig. 4 the location awareness scene of the spot beam emitter

As the location awareness model has been achieved, on the basis of the analysis function of STK, the link budget report can be generated. Whenever the CubeSats receives the spot beam signals, the report recode time information, measurements and positions of the CubeSates. Data for verification of the location awareness algorithm can be obtained by this report.

4. Simulation Results and Analysis

The location awareness model of the spot beam emitters is run for one day in the STK. The data used to verify the location algorithm are obtained from the location awareness model. PF and Extended Kalman Filter (EKF) are utilized to obtain an estimate of the position of the spot beam emitters. The angle measurement errors are set to $\delta_\beta = 0.1°$ and $\delta_\varepsilon = 0.1°$, while the frequency measurement error to $\delta_f = 100\text{Hz}$. The sampling time T is chosen as 1s. For the number of samples N = 3000 is used in PF, and the threshold for resampling is set to $N_{thres} = N/3$.

In the first trial, we compare the location results of Ku-band spot beam emitters based on a single CubeSat with that based on four CubeSats. Whenever the CubeSat detects the spot beam signals, the position of the CubeSat and the position of the spot beam emitters estimated by PF are simulated. Figure 5 shows the location awareness results with a single CubeSat, where the symbol (*) represents the position of the CubeSat when CubeSat detects the signal, the symbol (*) represents the position of the G-28 emitter estimated by PF when the CubeSat detects the G-28 beam 1, the symbol (○) represents the position of the AMSC1 emitter estimated by PF when the CubeSat detects the AMSC1 beam 1, the symbol (△) represents the position of the AMSC1 emitter estimated by PF when the CubeSat detects the AMSC1 beam 2. It illustrates that a single CubeSat can effectively identify the position of the spot beam emitters. However, a single CubeSat can only detect at most two spot beams. It is impossible to complete the monitoring task for spot beam in any position. As comparison, the location awareness results with four CubeSats are simulated as Figure 6 shows, where symbols (*, +, ○, △) represent different positions of CubeSats when the different beam signals are detected, respectively. Furthermore, the symbol (*) represents the position of the G-28 emitter estimated by PF when the CubeSat detects the G-28 beam 1, the symbol (+) represents the position of the G-28 emitter estimated by PF when the CubeSat detects the G-28 beam 2, the symbol (○) represents the position of the AMSC1 emitter estimated by PF when the CubeSat detects the AMSC1 beam 1, and the symbol (△) represents the position of the AMSC1 emitter estimated by PF when the CubeSat detects the AMSC1 beam 2. The simulation result shows that all four Ku-band spot beams are well detected and the corresponding positions of the spot beam emitters are estimated correctly.

The position and velocity root mean square errors (RMSE) versus time for different location algorithm are then examined in the second trial. The position and velocity

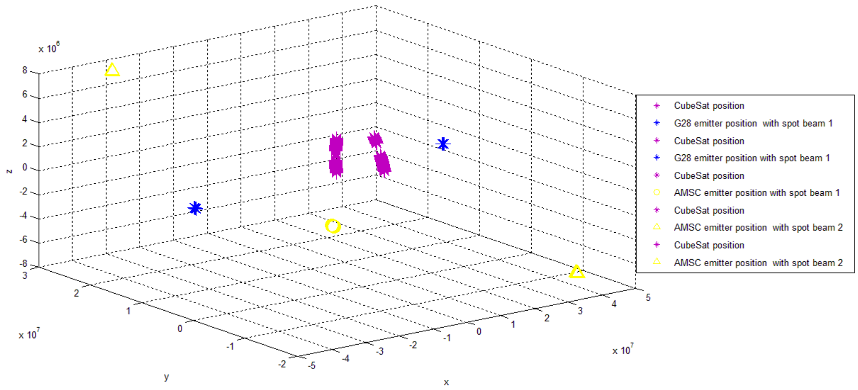

Fig. 5 the location awareness results of the spot beam emitters with single Ku-band CubeSat

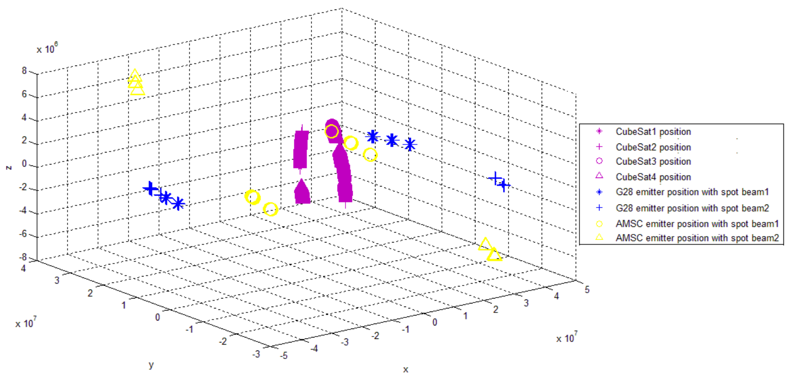

Fig. 6 the location awareness results of the spot beam emitters with four Ku-band CubeSat

RMSE are computed by equation (21) and (22).

$$P_{RMSE} = \sqrt{(\hat{x}_i - x_i)^2 + (\hat{y}_i - y_i)^2 + (\hat{z}_i - z_i)^2} \quad (21)$$

$$V_{RMSE} = \sqrt{(\widehat{v_x}_i - v_{x_i})^2 + (\widehat{v_y}_i - v_{y_i})^2 + (\widehat{v_z}_i - v_{z_i})^2} \quad (22)$$

where (x_i, y_i, z_i) and $(v_{x_i}, v_{y_i}\ v_{z_i})$ represent the position and velocity of the spot beam emitter at time *i* respectively. The position and velocity can be obtained from the STK model. The symbol (^) denotes location algorithm estimation. The angle-only, frequency-only and angle/frequency are compared on the basis of EKF and PF. According to the simulation results from the STK, the longest monitoring time of the Ku-band spot beam is 193s. The set of data is selected to verify the performance of the location algorithms. The position and velocity RMSE are simulated as Figure 7 and Figure 8 display.

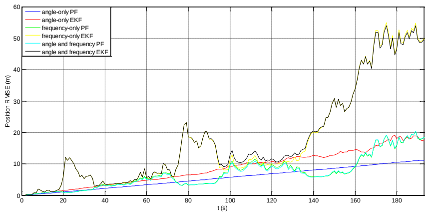

Fig. 7 position RMSE for the EKF and PF

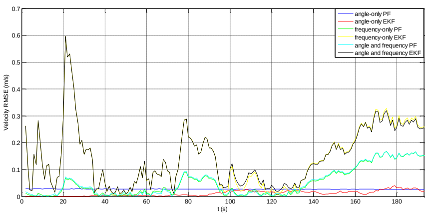

Fig.8 velocity RMSE for the EKF and PF

It is shown that the location awareness of the spot beam emitters can be accomplished by angle-only measurement, frequency-only measurement and angle/frequency joint measurement location algorithm. Under all kinds of measurement conditions, the estimation accuracy of PF is better than that of EKF. The position estimation error is less than 60m, whose magnitude is small enough for different spot beam emitters in space to be identified. Furthermore, the minor velocity RMSE is shown in Figure 8.

The location awareness results of the Ka-band spot beam emitters are analyzed in the final trial. It is shown that the CubeSats can detect all three Ka-band spot beams and estimate the position of the spot beams emitter, shown in Figure 9. Therefore, these trial results show that the proposed method is effective for location awareness of the spot beam emitters.

5. Conclusion

In this paper, a location awareness method based on a LEO CubeSat constellation is proposed for the efficient position identification of the spot beam emitters on a global scale. The properties such as geometry, the target motion equation, the measurement process and the Particle Filter equations are all addressed with respect to the location methods. To show the accuracy of our proposed method, a realistic scenario simulated within the STK is designed, in which CubeSats receive signals from the spot beam emitters. Our location awareness method is validated to be accurate by the simulation scenario. And the results have shown the feasibility of this method in the location awareness of the spot beam emitters.

6. Acknowledgments

This work is sponsored by the National Natural Science Foundation of China (Grant number: 61471021) and the China Academy of Launch Vehicle Technology Foundation.

7. References

[1] US. Government., 'National Security Space Strategy Unclassified Summary' (US Policy, 2011)
[2] ‘SDA Overview’, http://www.space-data.org/sda/about/sda-overview/, accessed 10 September 2017
[3] ‘DVB-CID’, http://satirg.org/dvb-cid/, accessed 25

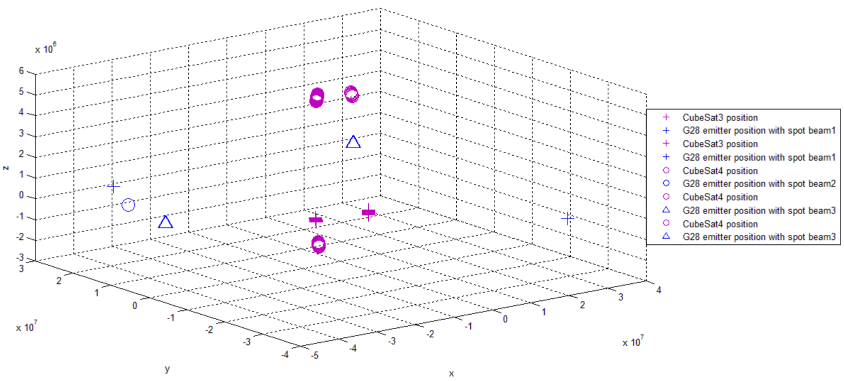

Fig. 9 the location awareness results of the spot beam emitters with four Ka-band CubeSat

6

September 2017
[4] Henri, Y.: 'ITU Radiomonitoring'. in ITU Asia-Pacific Regional Workshop on Satellite Launching & Coordination, Indonesia, 2013.
[5] Jacob, A. L., Jonathan, B.: 'A CubeSat Mission and Configuration Analysis for Locating and Mapping Spot Beams of Geostationary Comm-Satellites'. 53rd AIAA Aerospace Sciences Meeting, AIAA SciTech Forum, Kissimmee, Florida, January 2015.
[6] 'GOMSPACE', https://gomspace.com/news/gomspace-secures-new-innovation-project-from-.aspx, accessed 28 September 2017
[7] Allen, G. L., Kai, F. G.: 'Position and Velocity stimation Via Bearing Observations', IEEE Transactions on Aerospace & Electronic Systems, 1978, AES-14, (4), 564-577
[8]Sherry, E. H., Vincent, J. A.: 'Observability Requirements for Three-Dimensional Tracking via Angle Measurements', IEEE Transactions on Aerospace and Electronic Systems, 1985, AES-21, (2), 200-207
[9] Aidala, V. J.: 'Kalman Filter Behavior in Bearing-Only Tracking Applications', IEEE Transactions on Aerospace and Electronic Systems, 1979, AES-15, (1), 29-39
[10] Aidala, V. J., Nardona, S. C.: 'Biased Estimation Properties of the Pseudolinear Tracking Filter', IEEE Transactions on Aerospace and Electronic Systems, 1982, 18, (4), 432-441.
[11] Steven, C. N., Marcus L. G.: 'A Closed-Form Solution to Bearings-Only Target Motion Analysis'. IEEE Journal of Oceanic Engineering , 1997, 22, (1), 168-178
[12] Nardone, S. C., Allen L., Gong, K. F.: 'Fundamental Properties and Performance of Conventional Bearings-Only Target Motion Analysis', IEEE Transactions on Automatic Control, 1984, AC-29, (9), 775-787.
[13] Lecadre, J.-P., Jauffret, C.: 'On the Convergence of Iterative Methods for Bearings-Only Tracking', IEEE Transactions on Aerospace and Electronic Systems, 1999, 35, (3)
[14] Song, L. T., Speyer, J.: 'A Stochastic Analysis of a Modified Gain Extend Kalman Filter with Application to Estimation with Bearings Only Measurements', IEEE Transaction on Automatic Control, 1985, AC-30, (10), 940-949.
[15] Chan, Y.T., Towers, J. J.: 'Sequential Localization of a Radiating Source By Doppler-Shifted Frequency Measurements', IEEE Transactions on Aerospace and Electronic Systems, 1992, 28, (4)
[16] Nelson, D.J., McMahon, J.B.: 'Target Location from the Estimated Instantaneous Received Frequency', Proceedings of SPIE 2011, 8020, (19)
[17] Chan, Y.T., Rudnicki, S. W.: Bearings-Only and Doppler-Bearing Tracking Using Instrumental Variables, IEEE Transactions on Aerospace and Electronic Systems, 1992, 28, (4)
[18] Klaus B.: 'A General Approach to TMA Observability from Angle and Frequency Measurements', IEEE Transactions on Aerospace and Electronic Systems, 1996, 32, (1)
[19] Becker, K.: 'Three-Dimensional Target Motion Analysis using Angle and Frequency Measurements', IEEE Transactions on Aerospace and Electronic Systems, 2005, 41, (1)
[20] Ho K. C., Chan Y. T.: 'An Asymptotically Unbiased Estimator for Bearings-Only and Doppler-Bearing Target Motion Analysis', IEEE Transactions On Signal Processing, 2006, 54, (3)
[21] Claude, J., Pierre B.-B.: 'Denis Pillon. Multi Frequencies And Bearing Target Motion Analysis', Properties and Sonar Applications. International Conference on Information Fusion , 2008, 1-8
[22] Gordon, N. J., Salmon, D. J., Smith, A. F. M.: 'Novel Approach to Nonlinear/Non-Gaussian Bayesian State Estimation', IEE Proceedings-Radar & Signal Processing, 1993, 140, (2), 107-113.
[23] Sanjeev, A., Branko R.: 'Comparison of the Particle Filter with Range-Parameterised and Modified Polar EKFs for Angle-Only Tracking', In Signal and Data Processing of Small Targets 2000, Proceedings of SPIE 2000, 4048
[24] Rodrigues, C. V. S. Soares-Filho, W.: 'Particles Filter applied in the real-time bearings-only tracking problem of a sonar target', Journal of the Acoustical Society of America, 2008 , 123, (5), 3335
[25] Rajesh, R., Vanshaj, S., Rajiv K.: 'Spider monkey optimisation assisted particle filter for robust object tracking', IET Comput. Vis., 2017, 11 (3), pp. 207-219
[26] Vallado, D.: 'Fundamentals of Astrodynamics and Applications', (3rd ed.), New York, NY and Hawthorne, 'Springer and Microcosm Press', 2007
[27] Glennon, E., Gauthier, J., Choudhury, M., *et al* : 'Project Biarri amd the Namuru V3.2 Spaceborne GPS Receiver', International Global Navigation Satellite Systems Society (IGNSS) Symposium, Outrigger Gold Coast, Australia, July 2013.
[28] 'Satbeams', http://www.satbeams.com, accessed 6 September 2017
[29] Horak, R.: 'Telecommunications and Data Communications Handbook', Hoboken, NJ: John Wiley & Sons, 2012